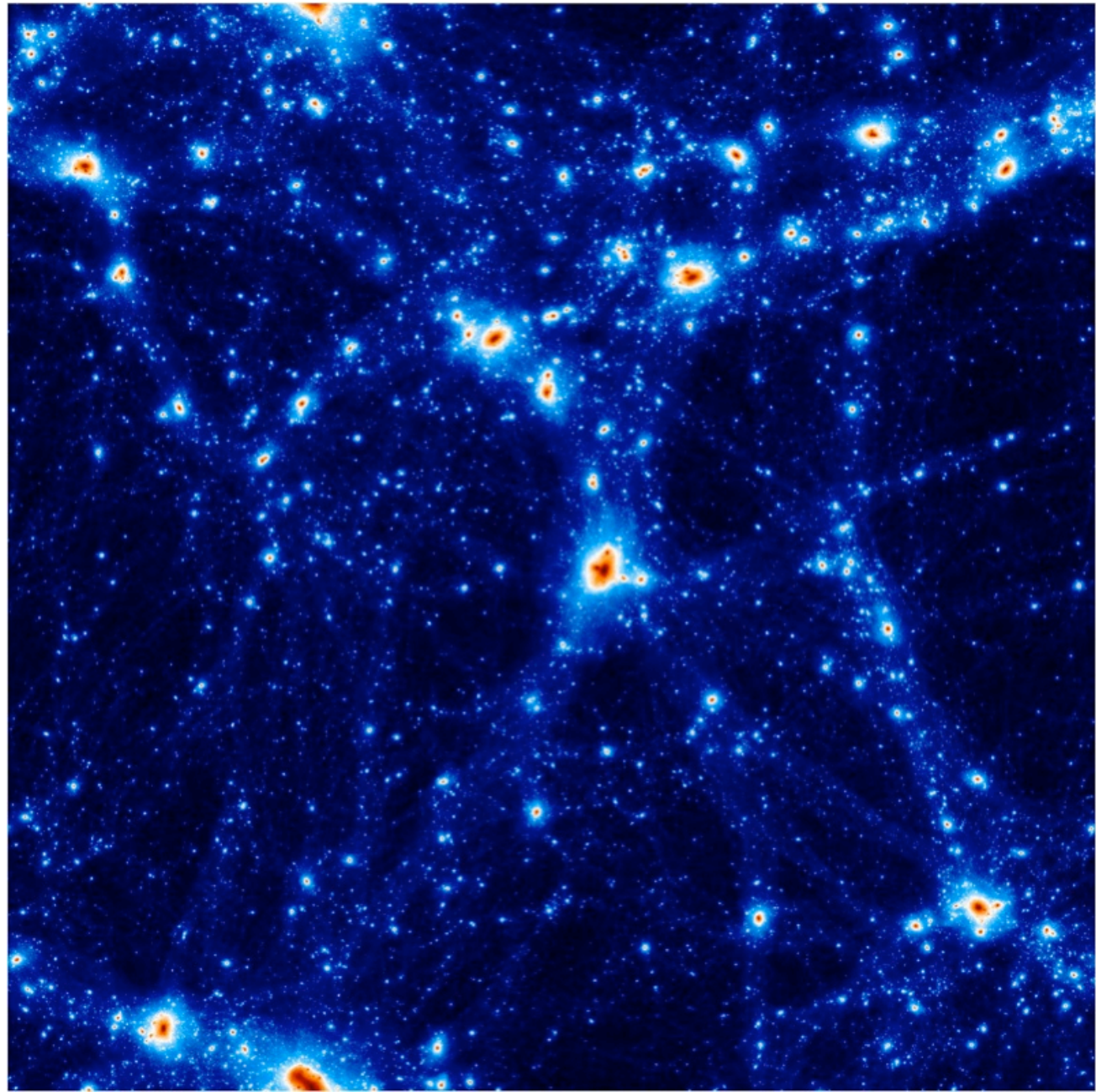


Francis Bernardeau
IPhT Saclay, France

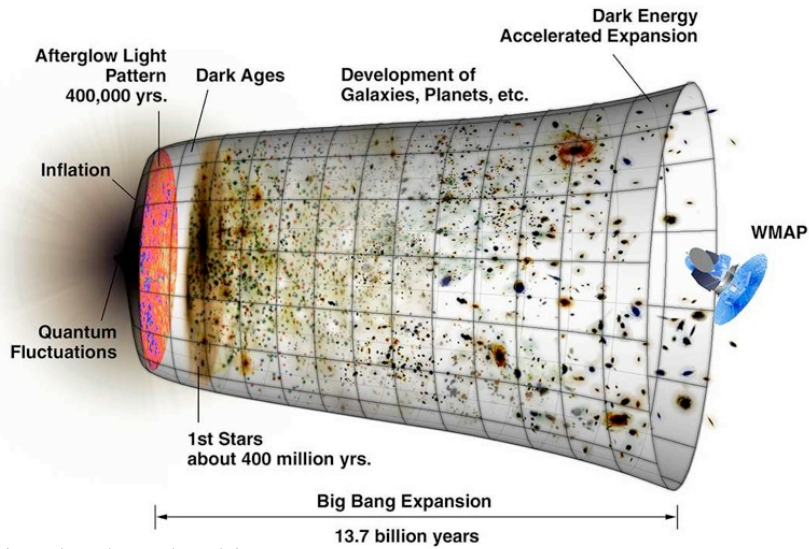
New methods to study the development of gravitational instabilities

COSMO/CosPA 2010 Tokyo



Outline

- ▶ Observables in large-scale structure surveys
 - ▶ *Historical perspectives and scientific objectives*
- ▶ A self-gravitating expanding dust fluid, evolution equations
 - ▶ *Results from standard perturbation theory calculations*
- ▶ A field theory reformulation of the evolution equations
 - ▶ *The closure and time-flow equations*
- ▶ The RPT reformulation of the perturbative series
 - ▶ *Insights into higher order propagators*
- ▶ Using large-scale structure observations to test gravity



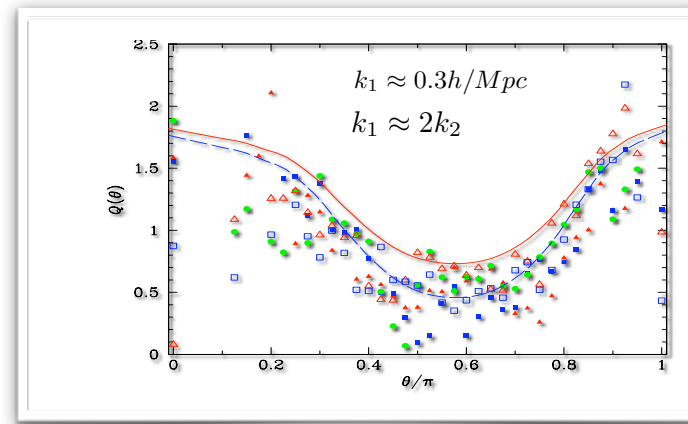
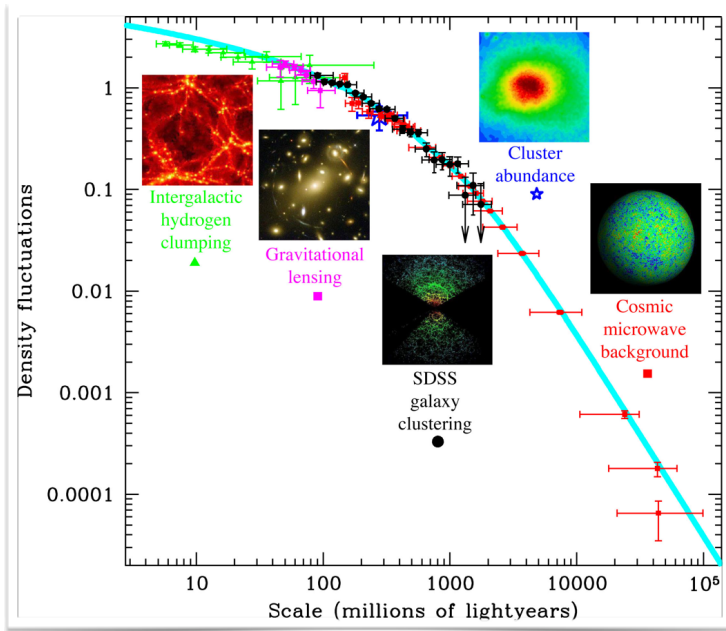
Which observables ?

$$\langle \delta_x(\mathbf{k}_1) \delta_x(\mathbf{k}_2) \delta_x(\mathbf{k}_3) \rangle = (2\pi)^3 \delta_{\text{Dirac}}(\mathbf{k}_1 + \mathbf{k}_2 + \mathbf{k}_3) B_x(\mathbf{k}_1, \mathbf{k}_2, \mathbf{k}_3)$$

and Bispectra

$$\langle \delta_x(\mathbf{k}_1) \delta_x(\mathbf{k}_2) \rangle = (2\pi)^3 \delta_{\text{Dirac}}(\mathbf{k}_1 + \mathbf{k}_2) P_x(k_1)$$

Power spectra



What for?

- ▶ Dark energy equation of state
- ▶ Neutrino mass
- ▶ Primordial NG (f_{NL} parameters)
- ▶ Testing gravity

Two regimes of interest

- ▶ accurate position measurements of the BAO at very large scales
- ▶ accurate description of the (poly)-spectra when it enters the quasi-linear regime

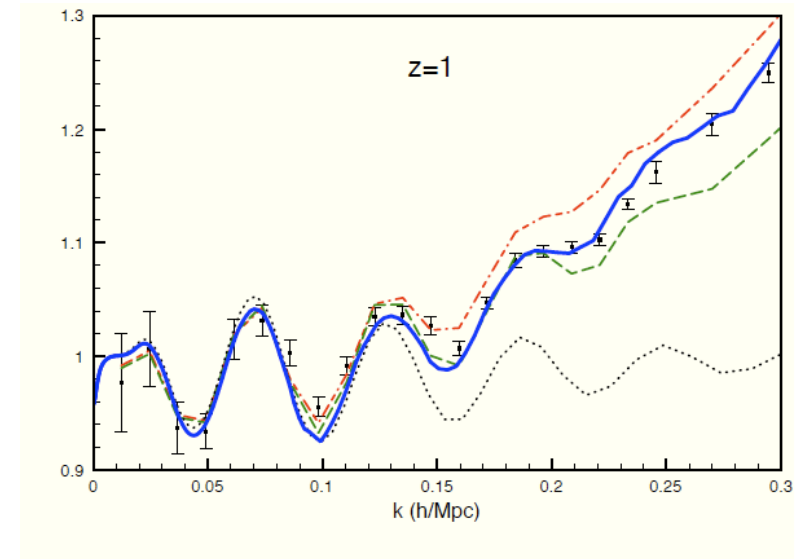
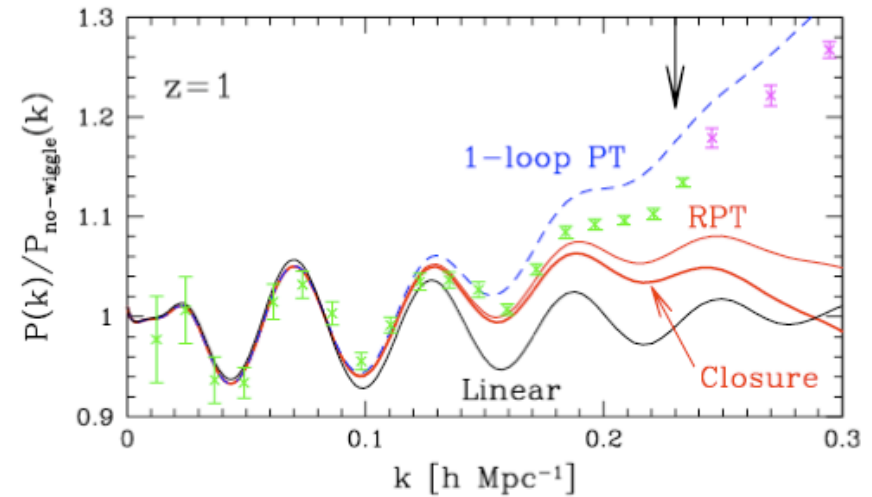
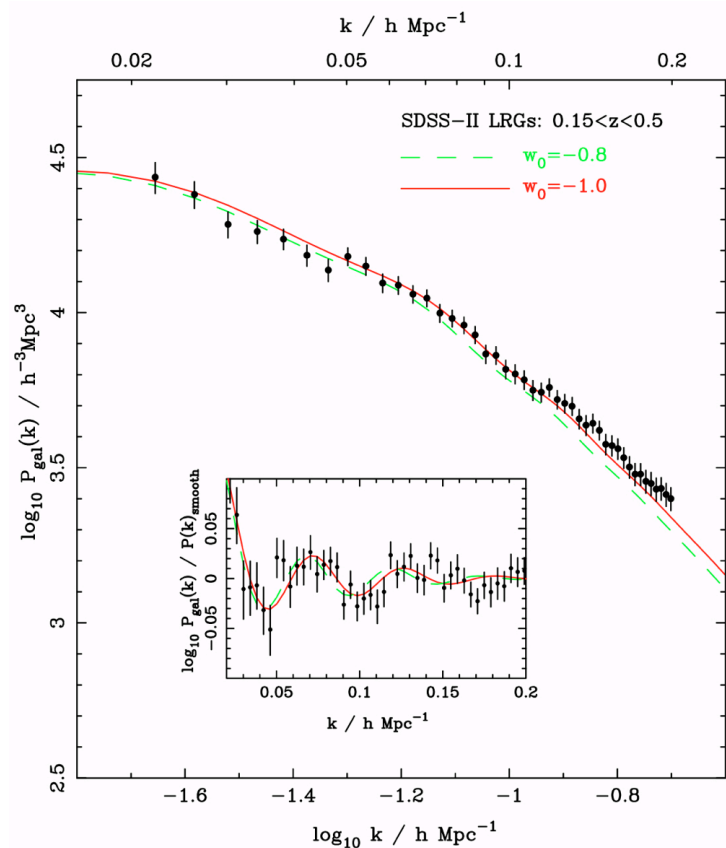


Figure 4. Power spectra at redshift $z = 1$ (divided by a smooth one). The continuous line is the result of the present paper, compared with linear theory (dotted), 1-loop PT (dash-dotted), the halo approach of ref. [20] (dashed). The dots with error bars are taken from the N -body simulation of ref. [10]. The background cosmology is a spatially flat Λ CDM model with $\Omega_{\Lambda}^0 = 0.73$, $\Omega_b^0 = 0.043$, $h = 0.7$, $n_s = 1$, $\sigma_8 = 0.8$.

A self-gravitating expanding dust fluid

A self-gravitating expanding dust fluid

- Data show that large-scale structure has formed from small density inhomogeneities since time of matter dominated universe with a dominant cold dark matter component

The Vlasov equation (collisionless Boltzmann equation) - $f(\mathbf{x}, \mathbf{p})$
is the phase space density distribution - are fully nonlinear.

$$\frac{df}{dt} = \frac{\partial}{\partial t} f(\mathbf{x}, \mathbf{p}, t) + \frac{\mathbf{p}}{ma^2} \frac{\partial}{\partial \mathbf{x}} f(\mathbf{x}, \mathbf{p}, t) - m \frac{\partial}{\partial \mathbf{x}} \Phi(\mathbf{x}) \frac{\partial}{\partial \mathbf{p}} f(\mathbf{x}, \mathbf{p}, t) = 0$$

$$\Delta \Phi(\mathbf{x}) = \frac{4\pi Gm}{a} \left(\int f(\mathbf{x}, \mathbf{p}, t) d^3 \mathbf{p} - \bar{n} \right)$$

This is what N-body codes aim at simulating...

The rules of the game:
single flow equations

*Peebles 1980; Fry 1984
FB, Colombi, Gaztañaga,
Scoccimarro, Phys. Rep.
2002*

$$\begin{aligned} \frac{\partial}{\partial t} \delta(\mathbf{x}, t) + \frac{1}{a} \nabla_i \cdot [(1 + \delta(\mathbf{x}, t)) \mathbf{u}_i(\mathbf{x}, t)] &= 0 \\ \frac{\partial}{\partial t} \mathbf{u}_i(\mathbf{x}, t) + \frac{\dot{a}}{a} \mathbf{u}_i(\mathbf{x}, t) + \frac{1}{a} \mathbf{u}_j(\mathbf{x}, t) \mathbf{u}_{i,j}(\mathbf{x}, t) &= -\frac{1}{a} \nabla_i \Phi(\mathbf{x}, t) \\ \nabla^2 \Phi(\mathbf{x}, t) - 4\pi G \bar{\rho}(t) a^2 \delta(\mathbf{x}, t) &= 0. \end{aligned}$$

+ expansion with respect to initial density fields

$$\delta(\mathbf{x}, t) = \delta^{(1)}(\mathbf{x}, t) + \delta^{(2)}(\mathbf{x}, t) + \dots$$

*GR corrections effects:
Yoo et al., PRD, 2009
B, Bonvin, Vernizzi, PRD, 2010*

► Motion equations in Fourier space in the single flow approximation

$$\frac{1}{H} \dot{\delta}(k, t) + \theta(k, t) = - \int d^3 \mathbf{k}_1 d^3 \mathbf{k}_2 \delta_D(\mathbf{k} - \mathbf{k}_1 - \mathbf{k}_2) \times \alpha(\mathbf{k}_1, \mathbf{k}_2) \delta(\mathbf{k}_1, t) \theta(\mathbf{k}_2, t)$$

$$\frac{1}{H} \dot{\theta}(k, t) + (2 + \frac{\dot{H}}{H^2}) \theta(k, t) + \frac{3}{2} \Omega_m \delta_m(k, t) = - \int d^3 \mathbf{k}_1 d^3 \mathbf{k}_2 \delta_D(\mathbf{k} - \mathbf{k}_1 - \mathbf{k}_2) \times \beta(\mathbf{k}_1, \mathbf{k}_2) \theta(\mathbf{k}_1) \theta(\mathbf{k}_2)$$

$$\alpha(\mathbf{k}_1, \mathbf{k}_2) = \frac{\mathbf{k}_{12} \cdot \mathbf{k}_1}{k_1^2} = 1 + \frac{\mathbf{k}_1 \cdot \mathbf{k}_2}{k_1^2}$$

$$\beta(\mathbf{k}_1, \mathbf{k}_2) = \frac{k_{12}^2 (\mathbf{k}_1 \cdot \mathbf{k}_2)}{2k_1^2 k_2^2} = \frac{(\mathbf{k}_1 \cdot \mathbf{k}_2)^2}{k_1^2 k_2^2} + \frac{\mathbf{k}_1 \cdot \mathbf{k}_2}{2k_1^2} + \frac{\mathbf{k}_1 \cdot \mathbf{k}_2}{2k_2^2}$$

- linear order = growth rate of structure
- higher order terms = mode couplings
- equations can be solved to any arbitrary order

$$\delta^{(n)}(\mathbf{k}) = \int d^3 \mathbf{k}_1 \dots d^3 \mathbf{k}_n \delta_D(\mathbf{k} - \mathbf{k}_{1\dots n}) \delta^{(1)}(\mathbf{k}_1) \dots \delta^{(1)}(\mathbf{k}_n) F_n^{(s)}(\mathbf{k}_1, \dots, \mathbf{k}_n)$$

$$\frac{\theta^{(n)}(\mathbf{k})}{f} = \int d^3 \mathbf{k}_1 \dots d^3 \mathbf{k}_n \delta_D(\mathbf{k} - \mathbf{k}_{1\dots n}) \delta^{(1)}(\mathbf{k}_1) \dots \delta^{(1)}(\mathbf{k}_n) G_n^{(s)}(\mathbf{k}_1, \dots, \mathbf{k}_n)$$

$$f \equiv \frac{d \log D_+}{d \log a}$$

... this is the reduced velocity divergence

- ▶ The kernels can be computed recursively...
- ▶ This is here the general form taken by the second order density field

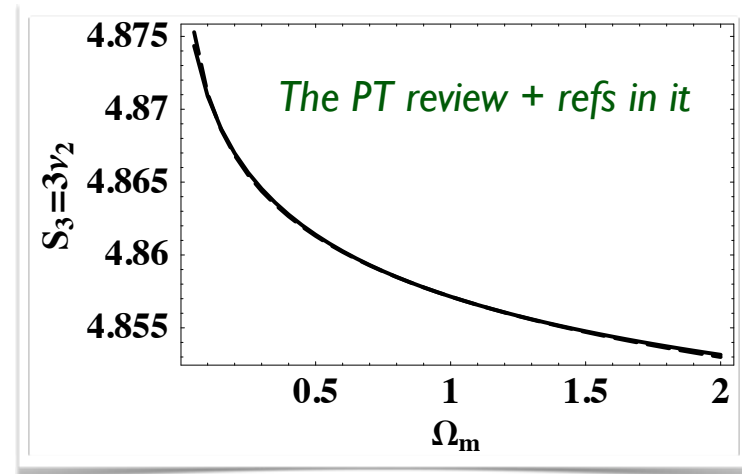
$$F_2^{(s)} = \left(\frac{3\nu_2}{4} - \frac{1}{2} \right) + \frac{1}{2} \frac{\mathbf{k}_1 \cdot \mathbf{k}_2}{k_1^2} + \frac{1}{2} \frac{\mathbf{k}_1 \cdot \mathbf{k}_2}{k_2^2} + \left(\frac{3}{2} - \frac{3\nu_2}{4} \right) \frac{(\mathbf{k}_1 \cdot \mathbf{k}_2)^2}{k_1^2 k_2^2}$$

This shape is expected (for CDM) irrespectively of background evolution, neutrino mass, etc...

$$\nu_2(\Omega_m, \Omega_\Lambda, \omega, \dots) = \frac{34}{21} + \dots$$

Einstein-de Sitter case

Flat universe: $\nu_2 = \frac{4}{3} + \frac{2}{7} \Omega_m^{-1/143}$



▶ Related observables (cosmic shear, redshift galaxy catalogues)

Observations are closely related (through projections, shape integration) to the density and the reduced velocity divergence power spectra and bispectra

- ▶ *inflation provides us with a compelling framework for the origin of such density fluctuations with specific statistics (Gaussian) and spectrum (nearly scale invariant before horizon crossing)*

► A lot is known at tree order

The *tree order* bispectra

$$B_\delta(\mathbf{k}_1, \mathbf{k}_2, \mathbf{k}_3) = \langle \delta^{(1)}(\mathbf{k}_1) \delta^{(1)}(\mathbf{k}_2) \delta^{(2)}(\mathbf{k}_3) \rangle + \text{sym.} = F_2^{(s)}(\mathbf{k}_1, \mathbf{k}_2) P(k_1) P(k_2) + \text{sym.}$$

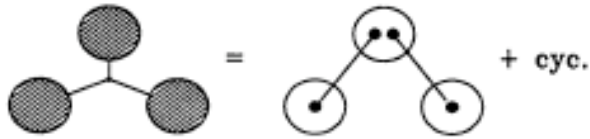


FIG. 3

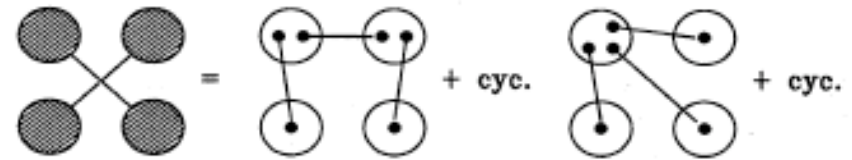
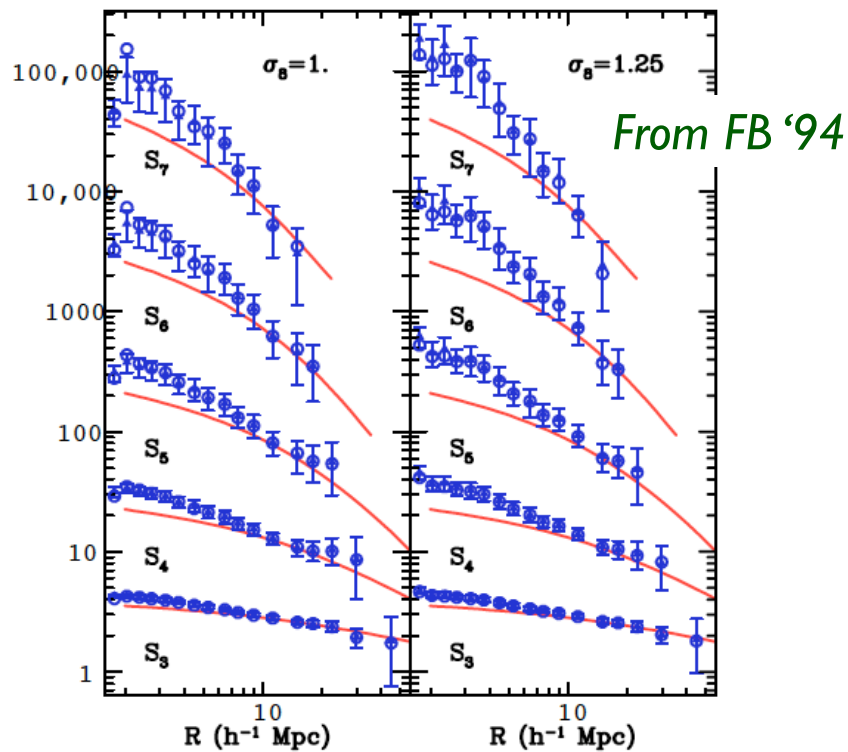
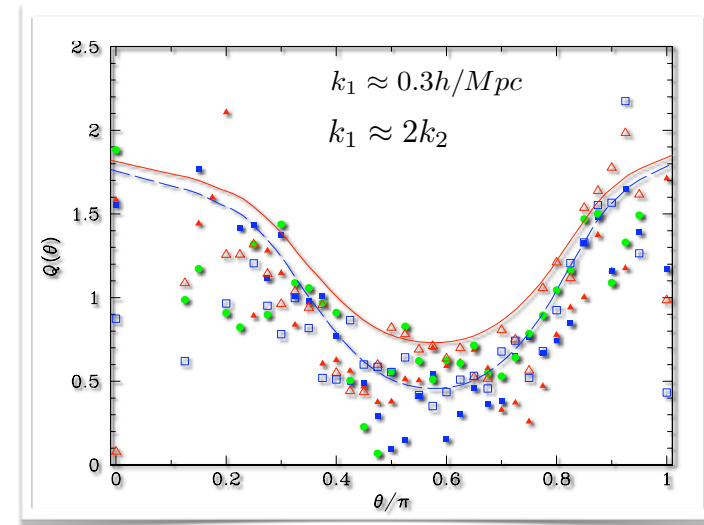


FIG. 4

Comparisons of poly-spectra (collapsed geometry) with N-body simulations...



... and in observations



From PSCz catalogue, Feldman et al.'01

- But things get not as nice when one wants to include loops

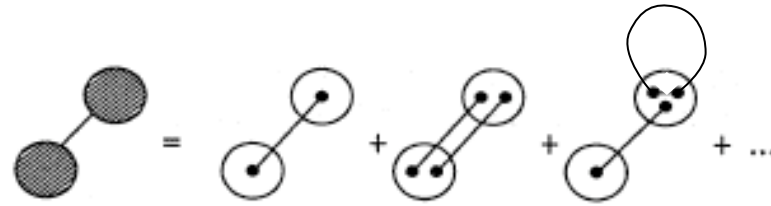


FIG. 2

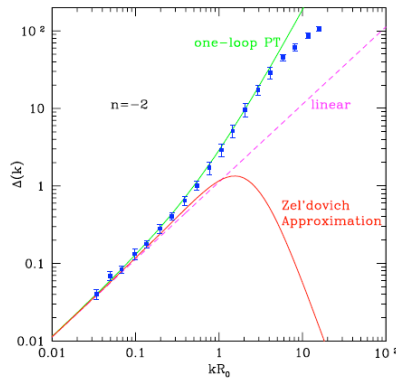
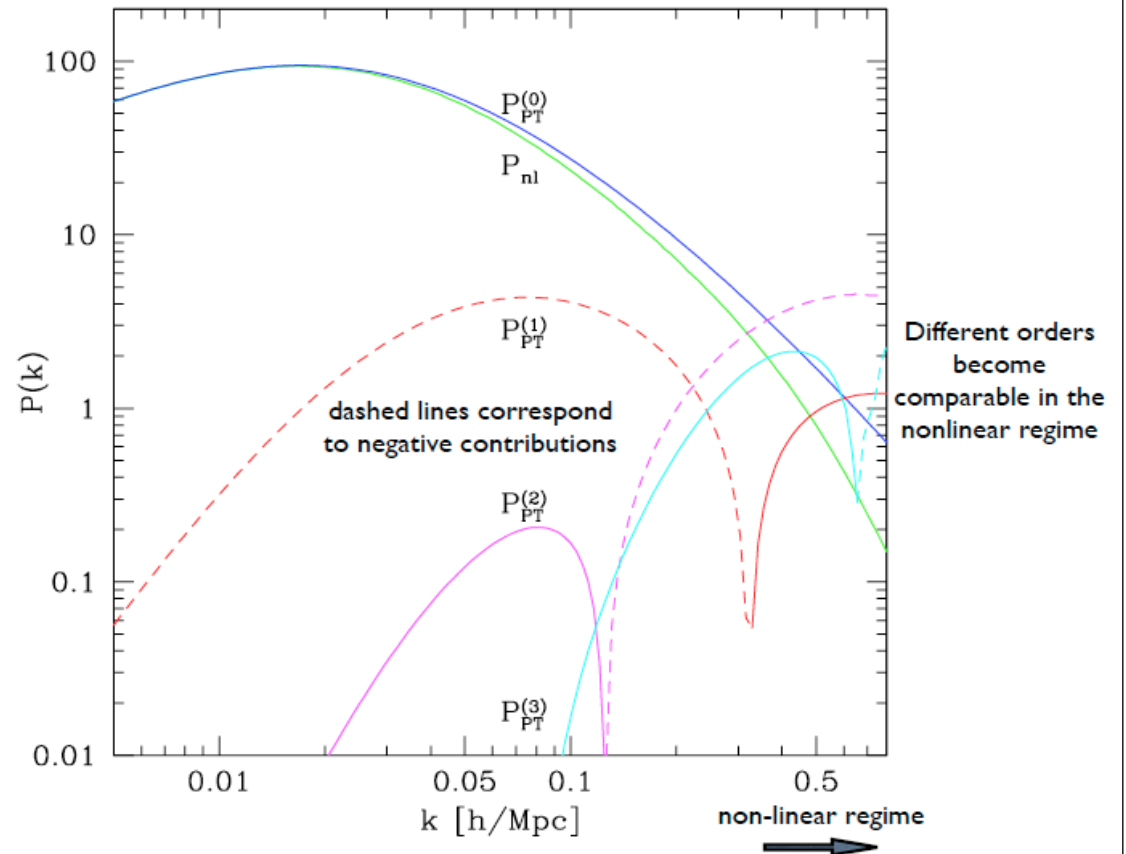


Fig. 13. The power spectrum for $n = -2$ scale-free initial conditions. Symbols denote measurements in numerical simulations from [560]. Lines denote linear PT, one-loop PT [Eq. (169)] and the Zel'dovich Approximation results [Eq. (181)], as labeled.



Not necessarily the best way to expand...

A field theory reformulation

Scoccimarro '97

A reformulation of the theory with a FT like approach

Scoccimarro '97

$$\Phi_a(\mathbf{k}, \eta) = g_{ab}(\eta)\Phi_b(\mathbf{k}, \eta = 0) + \int_0^\eta d\eta' g_{ij}(\eta - \eta')\gamma_{abcd}(\mathbf{k}_1, \mathbf{k}_2)\Phi_c(\mathbf{k}_1)\Phi_d(\mathbf{k}_2)$$

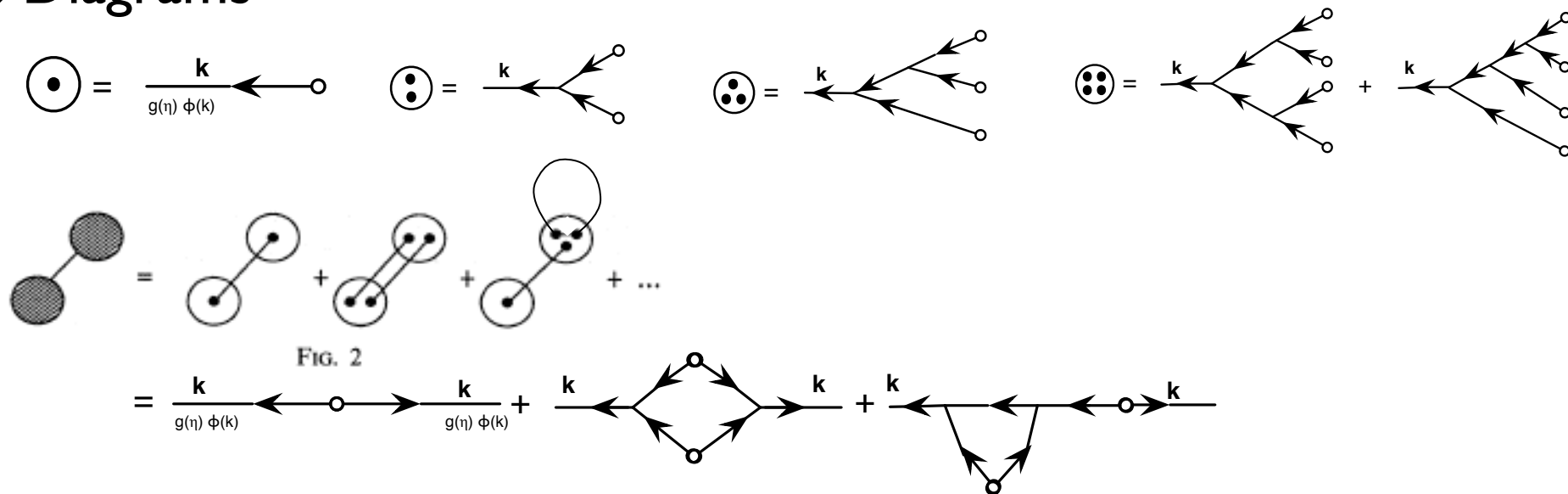
density-div v doublet

$$\begin{pmatrix} \delta(\mathbf{k}) \\ \theta(\mathbf{k}) \end{pmatrix}$$

doublet linear propagator

$$g_{ab}(\eta) = \frac{e^\eta}{5} \begin{bmatrix} 3 & 2 \\ 3 & 2 \end{bmatrix} - \frac{e^{-3\eta/2}}{5} \begin{bmatrix} -2 & 2 \\ 3 & -3 \end{bmatrix}$$

► Diagrams



Note : detailed effects of baryons versus DM can be taken into account (Somogyi & Smith 2010) with a 4-component multiplet, for neutrinos it is more complicated...

Not a standard quantum field theory problem...

- The observables are (or rather PDF of) expectation values that correspond to ensemble averages over the statistics of “initial” conditions (taken after decoupling).
- The system is not invariant over time translation: it is actually an unstable (non-equilibrium) system, where perturbations grow with time (as \sim power-law). The late time behavior of this system is probably non trivial and there is no known solution to it.
- Propagator has growing and decaying modes, both play important roles in the nonlinear regime. For standard (GR) cosmological models the model dependence is entirely encoded in the time dependence of the propagators.
- Loop corrections are not due to virtual particle productions but to mode couplings effects, modes being set in the initial conditions.
- Vertices have a non-trivial k -dependence but which is entirely due to the conservation equation and is independent of the energy content of the universe. Only $2 \rightarrow 1$ vertices exist (quadratic couplings). This is not the case generically for modified gravity models (like chameleon, DGP ...)
- Due to the shape of CDM spectrum, there are no UV divergences (nor IR). Loops, e.g. “Renormalizations”, are all finite.

Time-flow equations

M. Pietroni '08

From the field evolution equation to the spectra evolution equation

Exact evolution equation for the power spectra

$$\begin{aligned}
 P_{ab}(\mathbf{k}, \eta) &= g_{ac}(\eta) g_{bd}(\eta) P_{cd}(\mathbf{k}, \eta = 0) \\
 &+ \int_0^\eta d\eta' \int d^3q g_{ae}(\eta, \eta') g_{bf}(\eta, \eta') \\
 &\times [\gamma_{ecd}(\mathbf{k}, -\mathbf{q}, \mathbf{q} - \mathbf{k}) B_{fcd}(\mathbf{k}, -\mathbf{q}, \mathbf{q} - \mathbf{k}; \eta') \\
 &+ \gamma_{fcd}(\mathbf{k}, -\mathbf{q}, \mathbf{q} - \mathbf{k}) B_{ecd}(\mathbf{k}, -\mathbf{q}, \mathbf{q} - \mathbf{k}; \eta')]
 \end{aligned}$$

Approximate evolution equation for the bispectra assuming no trispectra

$$\begin{aligned}
 B_{abc}(\mathbf{k}, -\mathbf{q}, \mathbf{q} - \mathbf{k}; \eta) &= \\
 &g_{ad}(\eta) g_{be}(\eta) g_{cf}(\eta) B_{def}(\mathbf{k}, -\mathbf{q}, \mathbf{q} - \mathbf{k}; \eta = 0) \\
 &+ 2 \int_0^\eta d\eta' e^{\eta'} g_{ad}(\mathbf{k}, \eta, \eta') g_{be}(-\mathbf{q}, \eta, \eta') g_{cf}(\mathbf{q} - \mathbf{k}, \eta, \eta') \\
 &\times [\gamma_{dgh}(\mathbf{k}, -\mathbf{q}, \mathbf{q} - \mathbf{k}) P_{eg}(\mathbf{q}, \eta') P_{fh}(\mathbf{q} - \mathbf{k}, \eta') \\
 &+ \gamma_{egh}(-\mathbf{q}, \mathbf{q} - \mathbf{k}, \mathbf{k}) P_{fg}(\mathbf{q} - \mathbf{k}, \eta') P_{dh}(\mathbf{k}, \eta') \\
 &+ \gamma_{fgh}(\mathbf{q} - \mathbf{k}, \mathbf{k}, -\mathbf{q}) P_{dg}(\mathbf{k}, \eta') P_{eh}(\mathbf{q}, \eta')]
 \end{aligned}$$

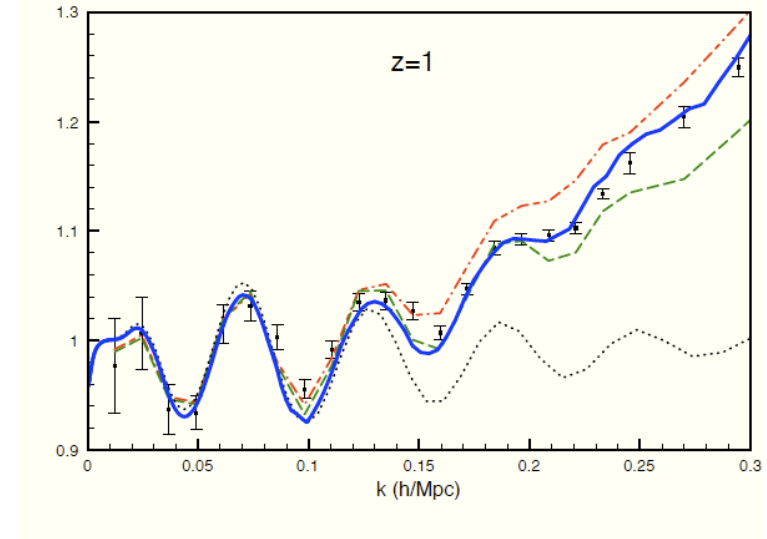


Figure 4. Power spectra at redshift $z = 1$ (divided by a smooth one). The continuous line is the result of the present paper, compared with linear theory (dotted), 1-loop PT (dash-dotted), the halo approach of ref. [20] (dashed). The dots with error bars are taken from the N -body simulation of ref. [10]. The background cosmology is a spatially flat Λ CDM model with $\Omega_\Lambda^0 = 0.73$, $\Omega_b^0 = 0.043$, $h = 0.7$, $n_s = 1$, $\sigma_8 = 0.8$.

The closure theory

It makes use of the unequal time power spectra

$$\langle \Phi_a(\mathbf{k}, \eta) \Phi_b(\mathbf{k}', \eta') \rangle = (2\pi)^3 \delta_{\text{Dirac}}(\mathbf{k} - \mathbf{k}') R_{ab}(k, \eta, \eta')$$

and of a non-linear propagator.

$$\left\langle \frac{\delta \Phi_a(\mathbf{k}, \eta)}{\delta \Phi_b(\mathbf{k}', \eta')} \right\rangle = G_{ab}(k, \eta, \eta') \delta_{\text{Dirac}}(\mathbf{k} - \mathbf{k}')$$

Then evolution equations for those quantities are derived using the Direct-Interaction (DI) approximation in which one separates the field expression in a DI part and a Non-DI part. At leading order in Non-DI \gg DI, one gets a set of closed equations,

$$\begin{aligned} \frac{\partial}{\partial \eta} R_{ab}(k, \eta, \eta') + \Omega_{ac} R_{cb}(k, \eta, \eta') = & \\ & \int_0^\eta d\eta'' M_{as}(k, \eta, \eta'') R_{bs}(k, \eta', \eta'') + \\ & \int_0^\eta d\eta'' N_{al}(k, \eta, \eta'') G_{bl}(k, \eta', \eta'') \\ \frac{\partial}{\partial \eta} G_{ab}(k, \eta, \eta') + \Omega_{ac} G_{cb}(k, \eta, \eta') = & \\ & \int_0^\eta d\eta'' M_{as}(k, \eta, \eta'') G_{bs}(k, \eta', \eta'') \end{aligned}$$

$$\begin{aligned} M_{as}(k, \eta, \eta'') = & \\ & 4 \int d^3 k' \gamma_{apq}(\mathbf{k} - \mathbf{k}', \mathbf{k}') \gamma_{lrs}(\mathbf{k}' - \mathbf{k}, \mathbf{k}) \\ & \times G_{ql}(k', \eta, \eta'') R_{pr}(|\mathbf{k} - \mathbf{k}'|, \eta, \eta'') \\ N_{al}(k, \eta, \eta'') = & \\ & 2 \int d^3 k' \gamma_{apq}(\mathbf{k} - \mathbf{k}', \mathbf{k}') \gamma_{lrs}(\mathbf{k}' - \mathbf{k}, \mathbf{k}) \\ & \times R_{qs}(k', \eta, \eta'') R_{pr}(|\mathbf{k} - \mathbf{k}'|, \eta, \eta'') \end{aligned}$$

These equations can more rigorously be derived in a large N expansion.

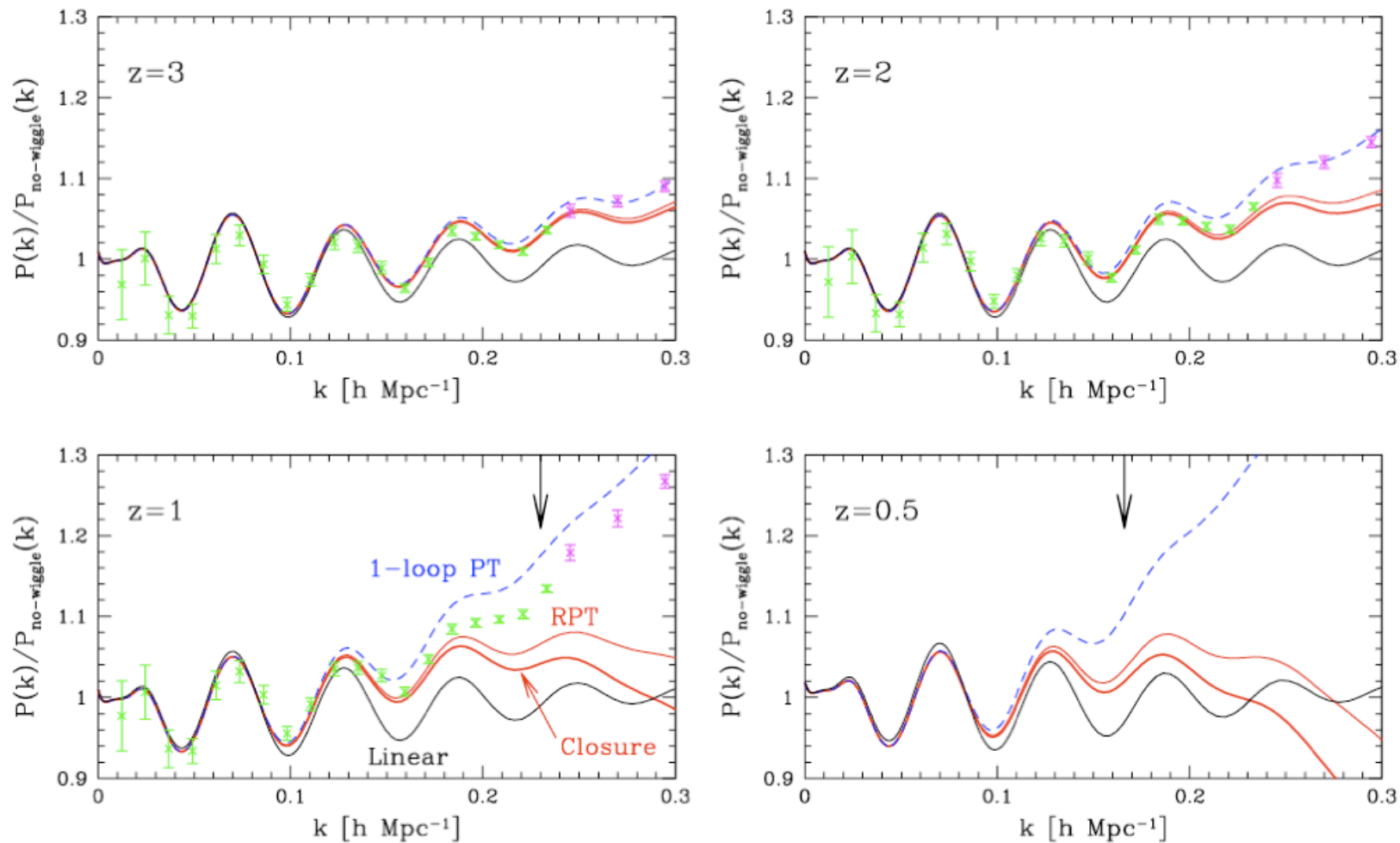


FIG. 3.— Ratio of non-linear power spectrum to smoothed linear spectrum, $P(k)/P_{\text{no-wiggle}}(k)$, given at specific redshifts, $z = 3, 2, 1$ and 0.5 . The error bar represents the N-body results taken from Jeong & Komatsu (2006), in which different color indicates the results with different box size (see their paper in detail). Here, smoothed linear spectra $P_{\text{no-wiggle}}(k)$ were calculated from the linear transfer function without baryon acoustic oscillation according to the fitting formula of Eisenstein & Hu (1998) (Eq.[29] of their paper). The non-linear power spectra are obtained from the first-order Born approximation to the integral solution (Eq.[64]), with approximate solutions of the non-linear propagator given by closure theory (thick) and RPT (thin). For comparison, one-loop predictions from the standard perturbation theory are plotted in dashed lines. Also, in panels with $z = 1$ and 0.5 , maximum wave number for limitation of one-loop perturbation is indicated by vertical arrows, according to the criterion, $\Delta^2(k) \equiv k^3 P(k)/(2\pi^2) \lesssim 0.4$ (Jeong & Komatsu 2006).

The RPT reformulation

One key ingredient : the propagator

Scoccimarro and Crocce PRD, 2005

$$G_{ab}(k, \eta) \delta_D(\mathbf{k} - \mathbf{k}') \equiv \left\langle \frac{\delta \Psi_a(\mathbf{k}, \eta)}{\delta \phi_b(\mathbf{k}')} \right\rangle$$

Final density / velocity div. \downarrow
 Initial Conditions \uparrow

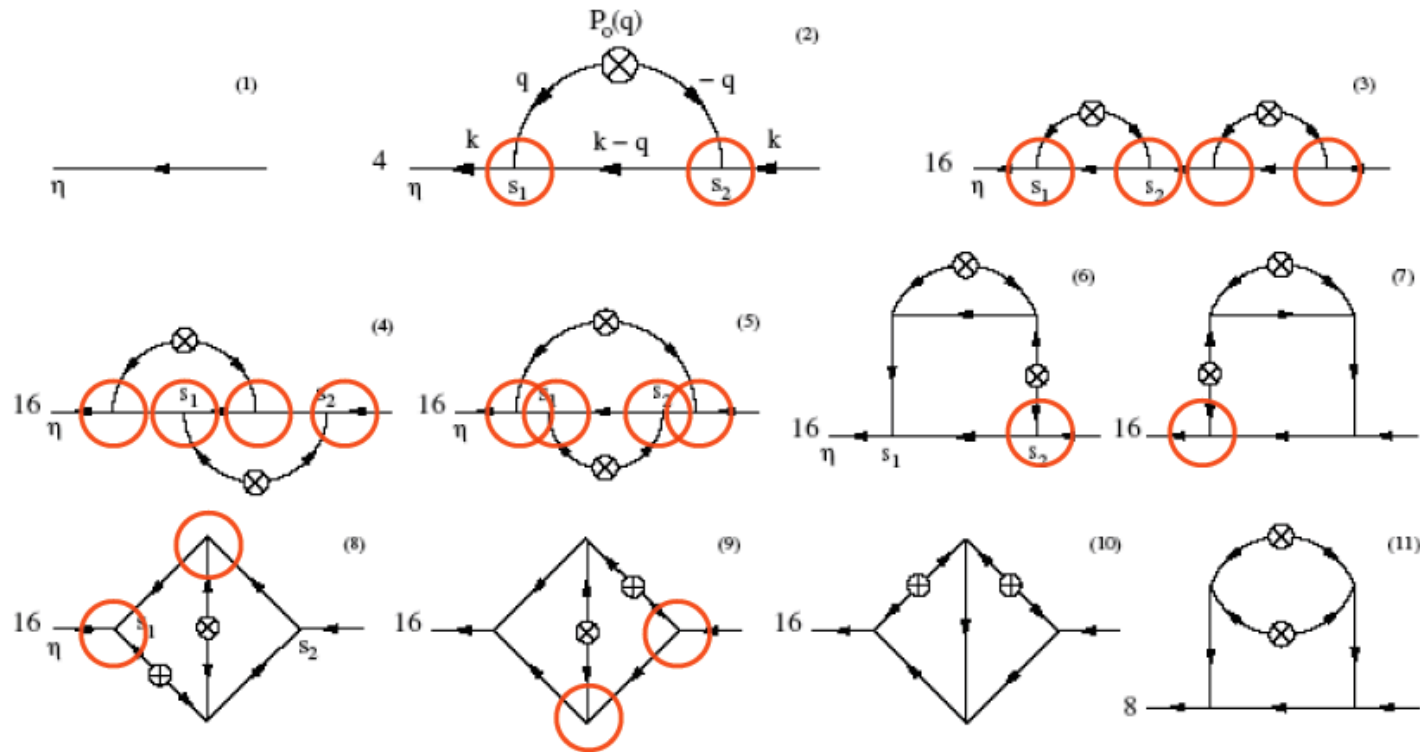


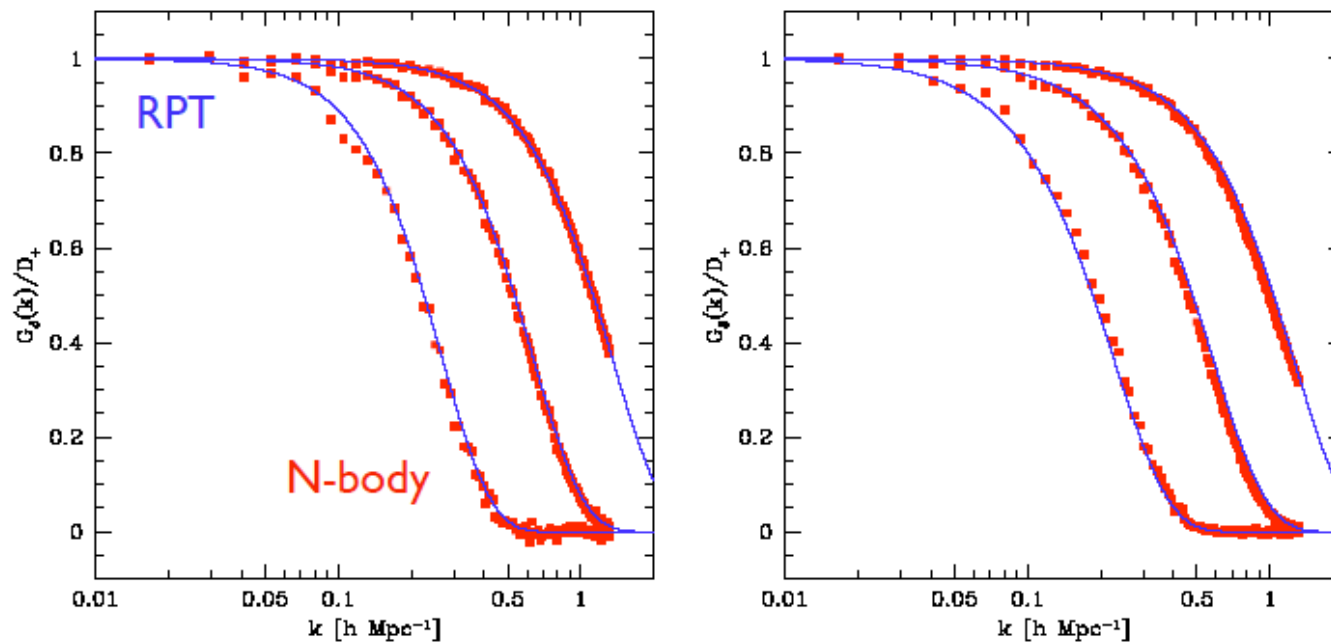
FIG. 2: Diagrams for the non linear propagator $G(k, \eta)$ up to two loops.

- ▶ The dominant contributions can be resummed exactly in the high k limit.

$$G_{ab}(k, \eta) \simeq g_{ab}(\eta) \exp\left(-\frac{1}{2}k^2\sigma_v^2(e^\eta - 1)^2\right) \quad (\text{high-}k \text{ limit})$$

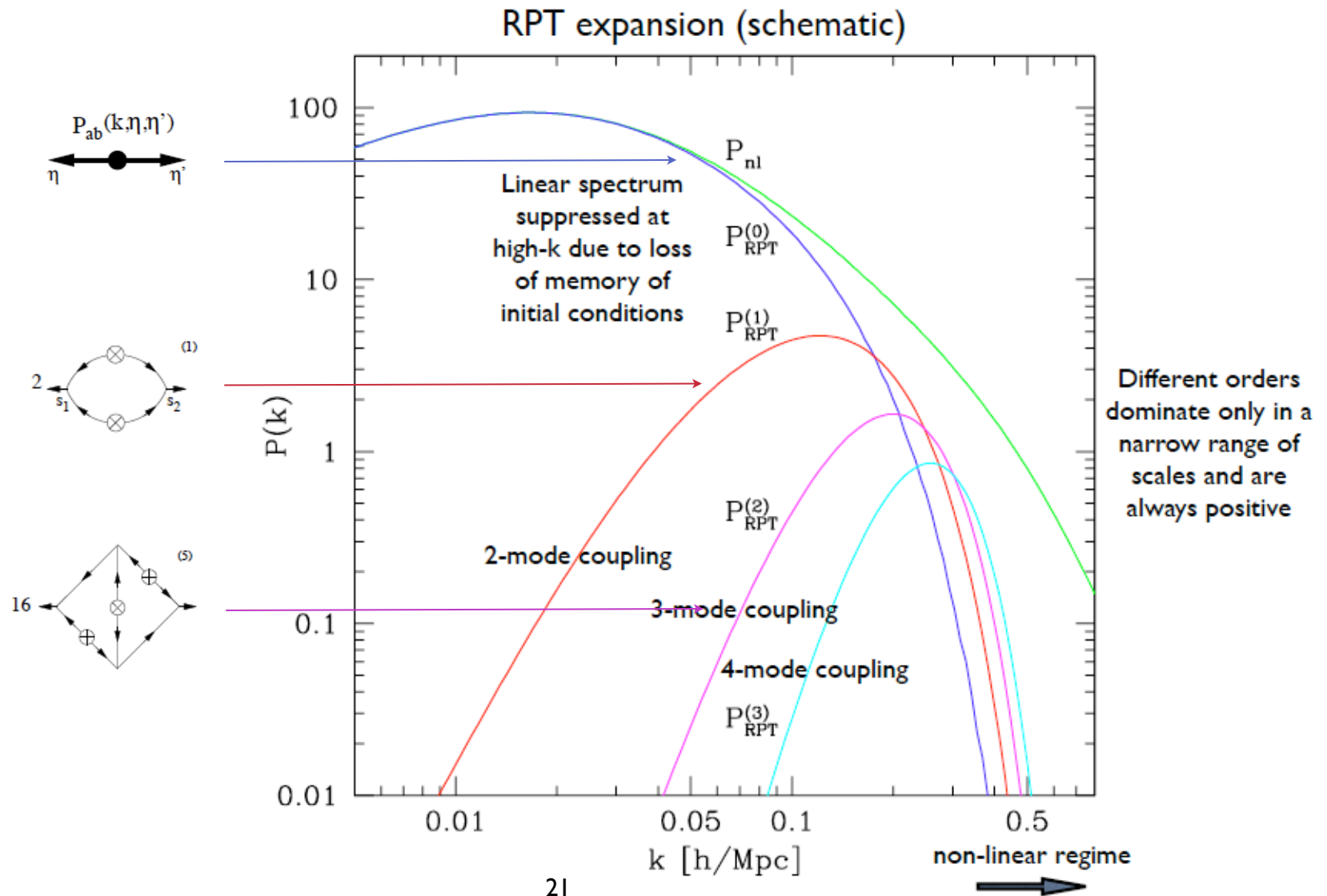
$$\sigma_v^2 \equiv \frac{1}{3} \int d^3q \frac{P(q)}{q^2}$$

Comparison between RPT and N-Body Simulations
($z = 0, 2, 5$)



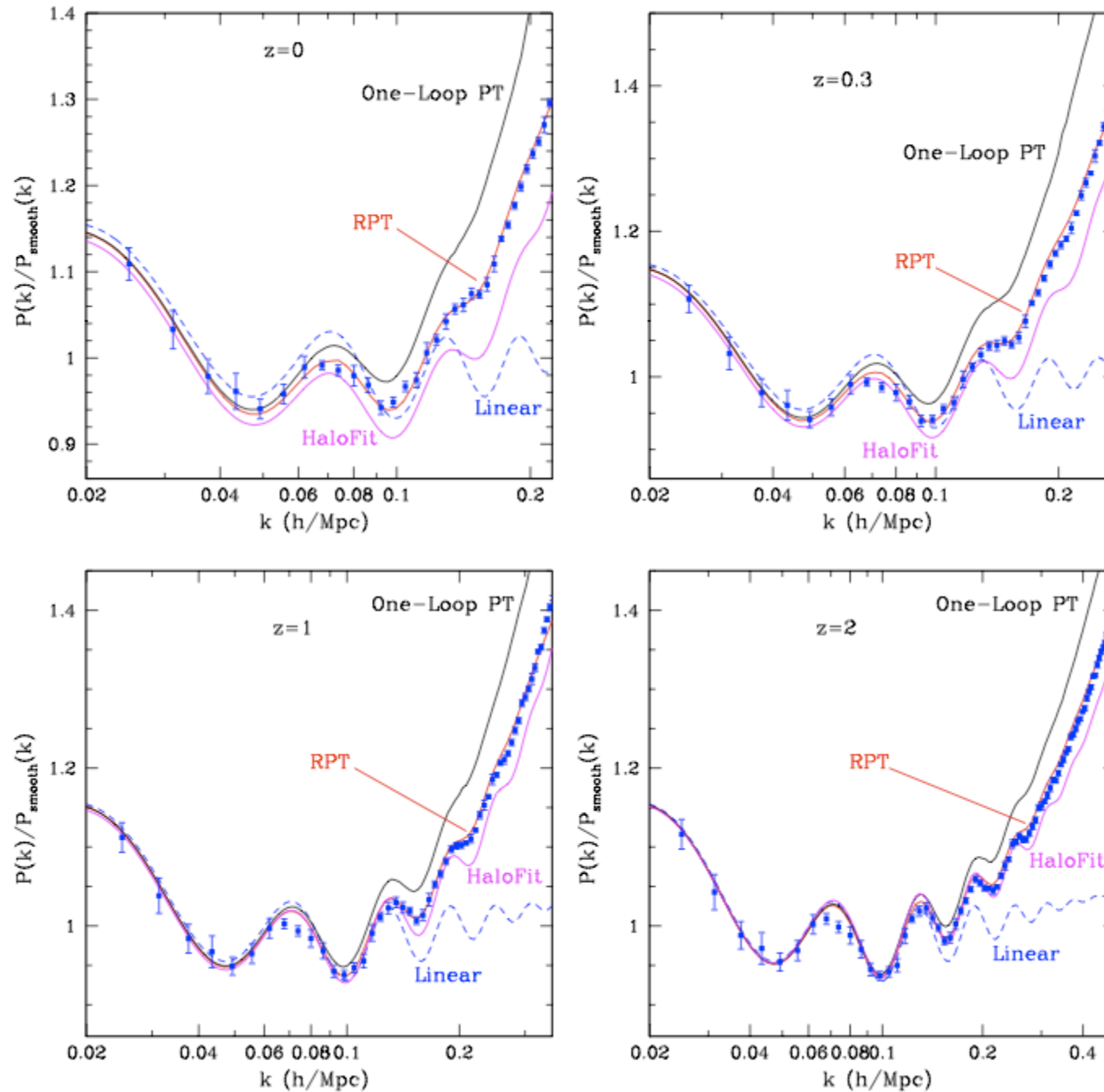
Crocce and Scoccimarro 05

► RPT (Scoccimarro and Crocce) consists in standard PT when $g \rightarrow G$



Evolution of baryonic oscillation with RPT

M. Crocce, R. Scoccimarro PRD, 2008



Insights into higher order propagators

► Towards a complete “renormalisation” of PT ?

FB, Croce, Scoccimarro, PRD, 2008

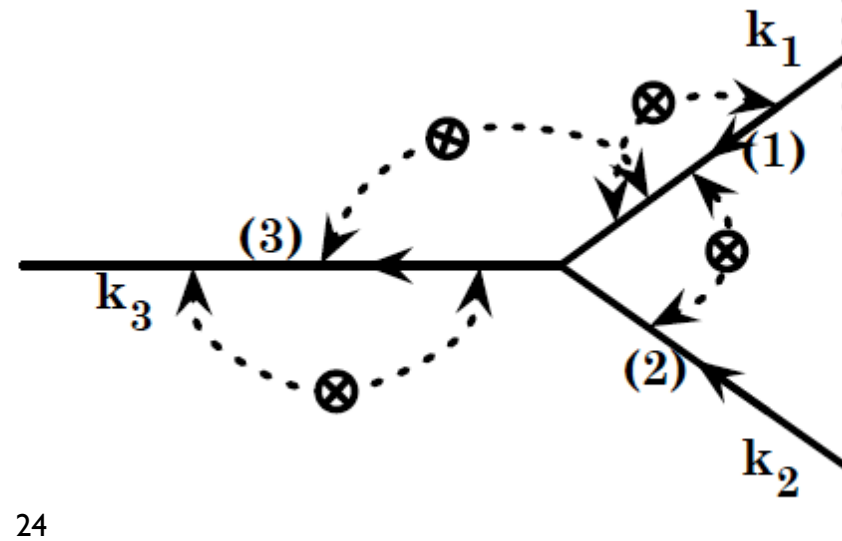
The next thing to look at is
the vertex ...



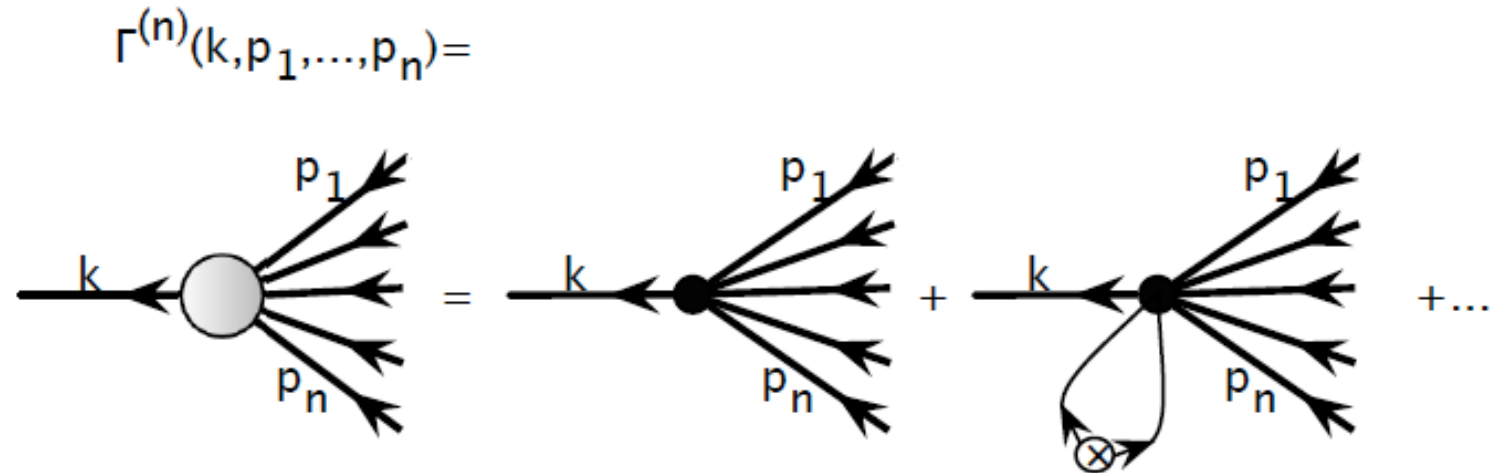
What we found is that these are the “p-point propagator” that can be
“renormalized”

$$\frac{1}{p!} \left\langle \frac{\delta^p \Psi_a(\mathbf{k}, \eta)}{\delta \phi_{b_1}(\mathbf{k}_1) \dots \delta \phi_{b_p}(\mathbf{k}_p)} \right\rangle = \delta_D(\mathbf{k} - \mathbf{k}_{1\dots p}) \Gamma_{ab_1\dots b_p}^{(p)}(\mathbf{k}_1, \dots, \mathbf{k}_p, \eta)$$

$$\Gamma_{abc}^{(2)}(\mathbf{k}_1, \mathbf{k}_2, \mathbf{k}_3)$$



- ▶ This suggests another scheme : use the n-point propagators as the building blocks



- ▶ The reconstruction of the power spectrum :

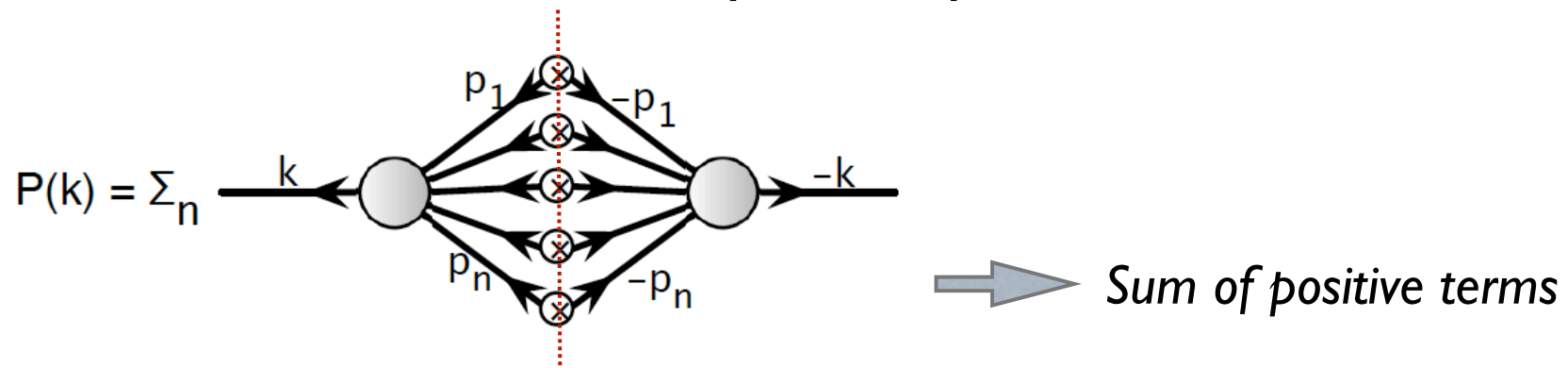
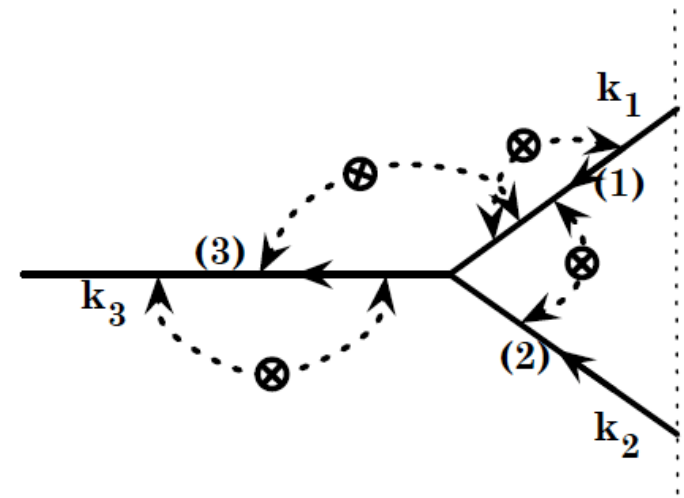


FIG. 3: Reconstruction of the power spectrum out of transfer functions. The crossed circles represent the initial power spectrum. The sum runs over the number of internal connecting lines, e.g. the number of such circles. It is to be noted that each term of this sum is positive.

► *Calculation of renormalized vertex in high k limit*



if p_{ij} is the number of lines connecting the segment (i) to (j)

$$\Gamma_{abc, \{p_{ij}\}}^{(2)} = \frac{s_{\{p_{ij}\}}}{\mathcal{M}_{\{p_{ij}\}}} \left(-\frac{\sigma_v^2}{4}\right)^{\sum_{i \leq j} p_{ij}} \prod_i k_i^{2p_{ii}} \prod_{i < j} (k_i \cdot k_j)^{p_{ij}} \int_0^s ds' g_{ad}(s-s') \gamma_{def}(k_1, k_2, k_3) g_{eb}(s') g_{fc}(s')$$

$$\times (e^{s'} - 1)^{2p_{11} + 2p_{22} + 2p_{12} + p_{13} + p_{23}} (e^s - e^{s'})^{2p_{33} + p_{13} + p_{23}} .$$

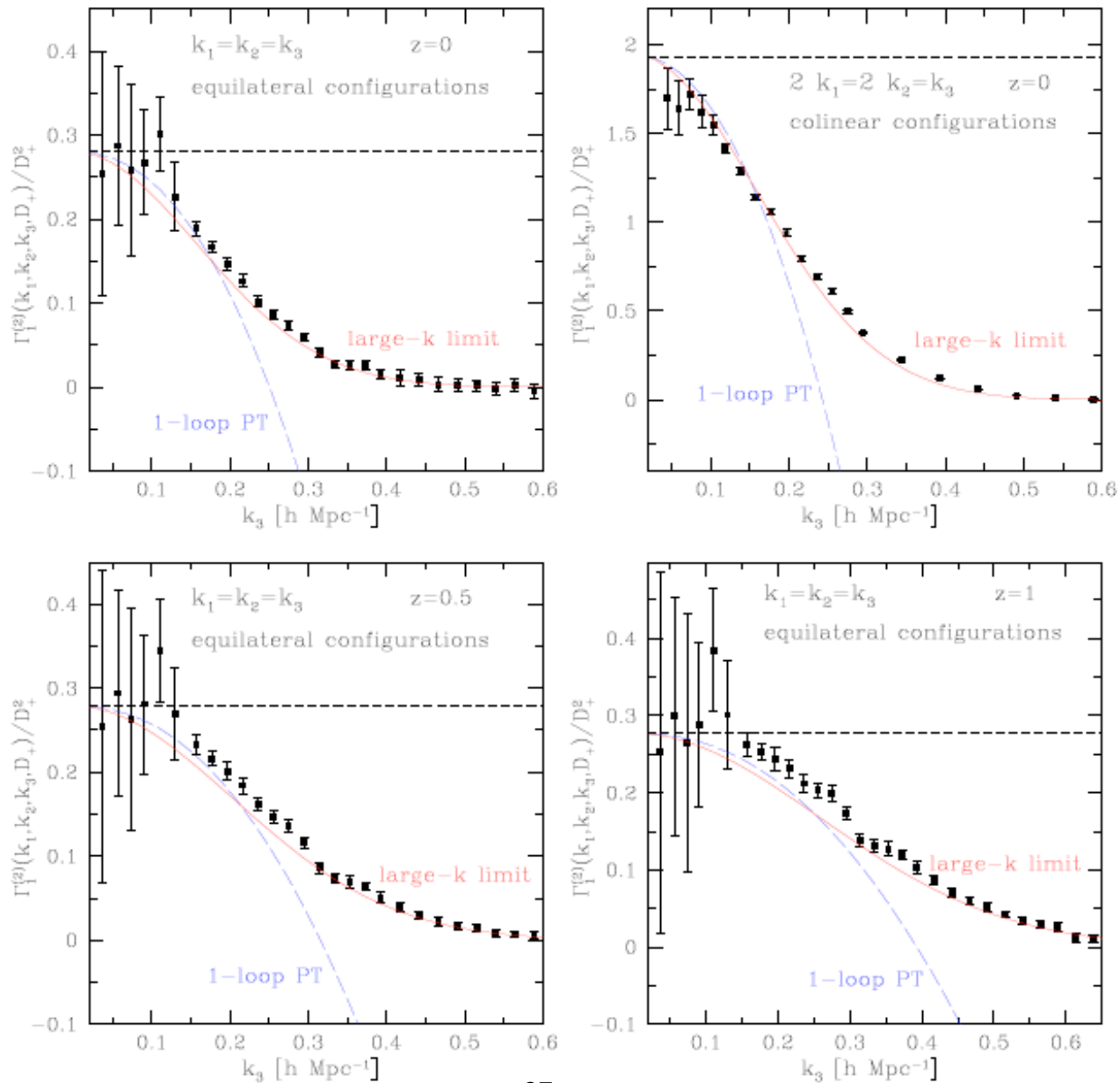
$$s_{\{p_{ij}\}} = 2^{\sum_{i \leq j} p_{ij}}$$

$$\mathcal{M}(p_{ii}) = 2^{p_{ii}} p_{ii}!, \text{ and } \mathcal{M}(p_{ij}) = p_{ij}! \text{ if } i \neq j$$

$$\Gamma_{abc}^{(2)}(k_1, k_2, k_3) = \exp\left(-\frac{\sigma_v^2 k_3^2}{2} (e^s - 1)^2\right) \Gamma_{abc, \text{tree}}^{(2)}$$

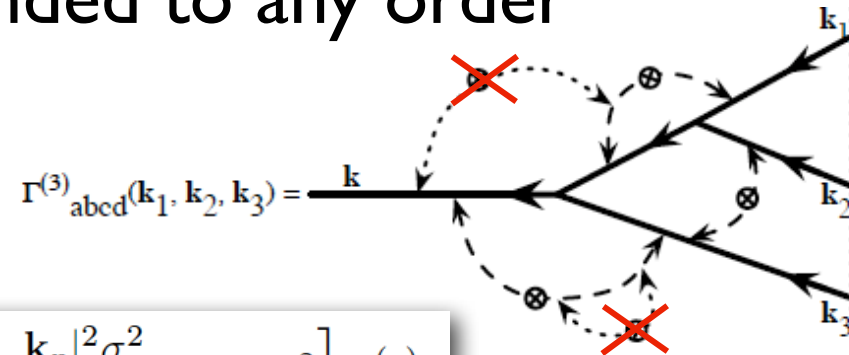
► *It implies that the vertex cannot be “renormalized” (into an operator which is local in time)*

Comparison with numerical simulations



► Re-summation can be extended to any order

FB, Crocce, Scoccimarro, PRD, 2008



In the large k limit we have :

$$\Gamma^{(p)} = \exp \left[-\frac{|\mathbf{k}_1 + \dots + \mathbf{k}_p|^2 \sigma_v^2}{2} (e^s - 1)^2 \right] \Gamma_{\text{tree}}^{(p)}$$

► Non-Gaussian initial conditions

Crocce, Sefusatti, FB, 2010

► The Gamma-expansion is still valid.

► In the large k limit we now have :

$$G(k) \rightarrow \exp \left[-\sum_{p=2}^{\infty} \frac{\langle (\mathbf{v} \cdot \mathbf{k})^p \rangle_c}{p!} (e^\eta - e^{\eta_0})^p \right]$$

instead of

$$G(k) \rightarrow \exp \left[-\frac{\langle (\mathbf{v} \cdot \mathbf{k})^2 \rangle_c}{2} (e^\eta - e^{\eta_0})^2 \right]$$

for Gaussian initial conditions.

- Does it speed up the convergence for the reconstruction of $P(k)$?
- Also provide the building blocks for higher order moments...

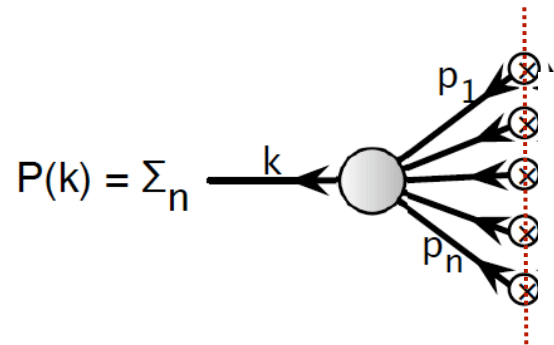
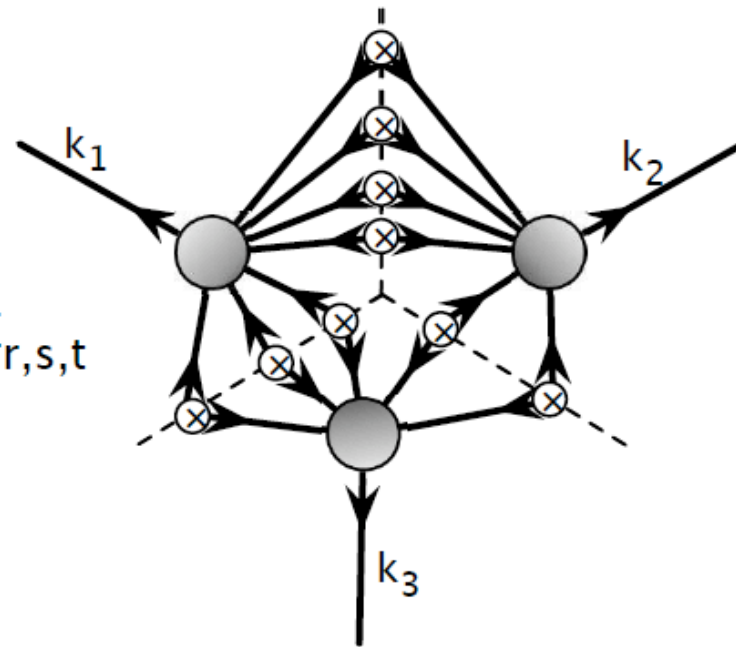
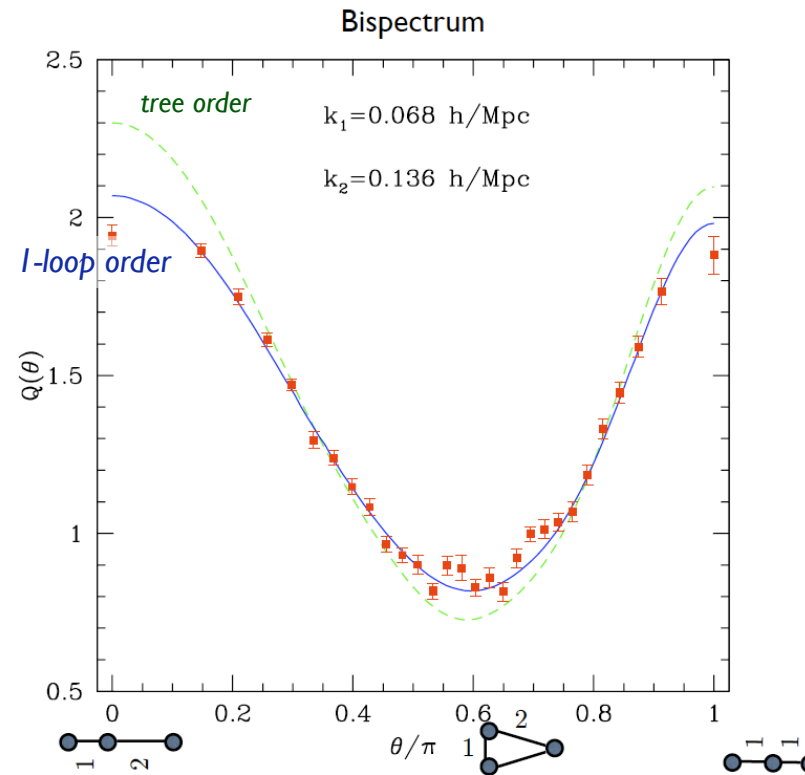


FIG. 3: Reconstruction of the power functions. The crossed circles represent spectrum. The sum runs over the numbering lines, e.g. the number of such circles that each term of this sum is positive.

$$B(k_1, k_2, k_3) = \sum_{r,s,t}$$



Application to bispectra



Measuring bispectra

- ▶ More information (hence better S/N) on mode amplitudes (all the more when one tries to exploit the quasi-linear or nonlinear regime, see [Rimes and Hamilton, MNRAS, 05](#))
- ▶ Intrinsic shape is a poor measurement of the energy content of the universe (e.g. dark energy equation of state) but can be used to test gravity

Using large-scale
structure to test
gravity

Changing gravity

There are many ways of doing so...

(Jain, Zhang PRD '08)

$$\frac{1}{H}\dot{\theta}(k) + \left(2 + \frac{\dot{H}}{H^2}\right)\theta(k) + \frac{3}{2}\Omega_m \xi(k, t) \delta_m(k) = \dots$$

If the change is such that

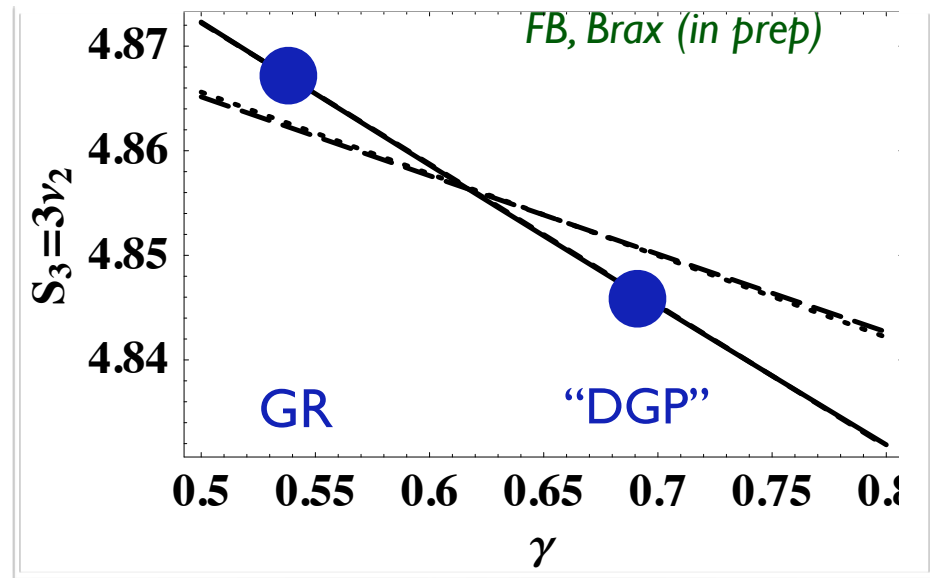
$$f_k \equiv \frac{d \log D_+}{d \log a} = \Omega_m^\gamma \quad (\gamma^{\text{GR}} \approx 0.55)$$

standard parameterization (Amendola & Quercellini, '04, Linder '05, Reyes et al. Nature, etc.),

$$\nu_2^{\text{MG}} = \nu_2^{\text{GR}} - \frac{10}{273}(\gamma - \gamma^{\text{GR}})(1 - \Omega_m)\Omega_m^{\gamma^{\text{GR}} - 1}$$

$$\mu_2^{\text{MG}} = \mu_2^{\text{GR}} - \frac{50}{273}(\gamma - \gamma^{\text{GR}})(1 - \Omega_m)\Omega_m^{\gamma^{\text{GR}} - 1}$$

This is still a modest change



In presence of a dilaton field

Brax et al. astro-ph/1005.3735

$$S = \int d^4x \sqrt{-g} \left\{ \frac{M_{\text{Pl}}^2}{2} \mathcal{R} - M_{\text{Pl}}^2 g^{\mu\nu} k^2(\phi) \partial_\mu \phi \partial_\nu \phi - V(\phi) \right\} + \int d^4x \sqrt{-\tilde{g}} \mathcal{L}_m(\psi_m^{(i)}, A^2(\phi) g_{\mu\nu}),$$

This extra field ϕ that is responsible of massive gravity effects. Its effect are suppressed in dense regions through the Chameleon mechanism.

$$A(\phi) = 1 + \frac{A_2}{2} (\phi - \phi_0)^2 + \dots$$

$$V(\phi) = A^4(\phi) V_0 \exp(-\phi)$$

$$k^2(\phi) = 3 \left(\frac{d \log A}{d\phi} \right)^2 + \frac{1}{\lambda^2}$$

A new force term:
$$F_i = -\frac{1}{a(t)} \left(\Phi(\mathbf{x}, t)_{,i} + \frac{d \log A}{d\phi} (\bar{\phi} + \delta\phi) \phi(\mathbf{x}, t)_{,i} \right)$$

Newton potentials, $\Phi = \Psi$ with standard Poisson equation

An effective potential for the dilaton field

$$V_{\text{eff.}}(\phi) = A^4(\phi) V_0 \exp(-\phi) + A(\phi) \rho_m \quad \frac{m_\phi^2}{H^2} \approx \frac{3A_2}{2} (\Omega_m + 4\Omega_\Lambda) \left[\lambda^{-2} + 3 \left(\frac{\Omega_m}{\Omega_\Lambda} + 4 \right)^{-2} \right]^{-1}$$

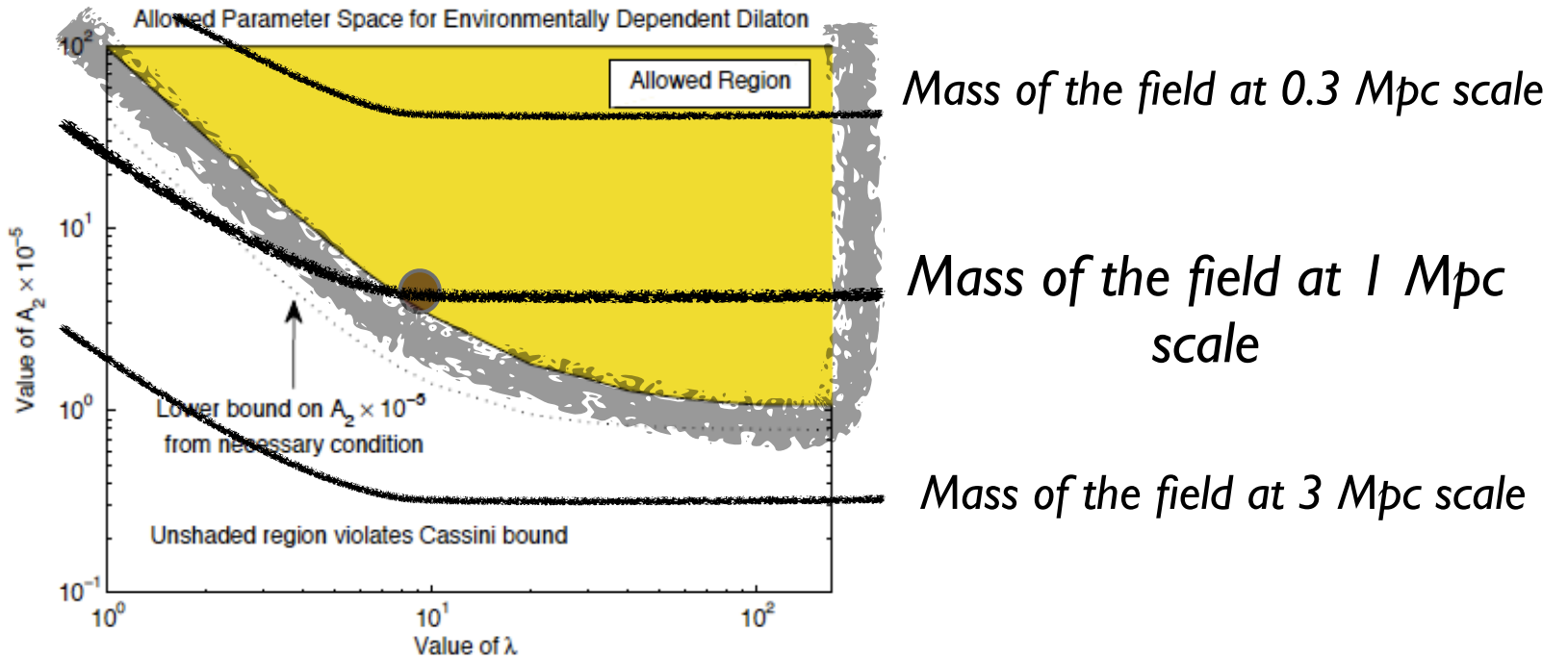
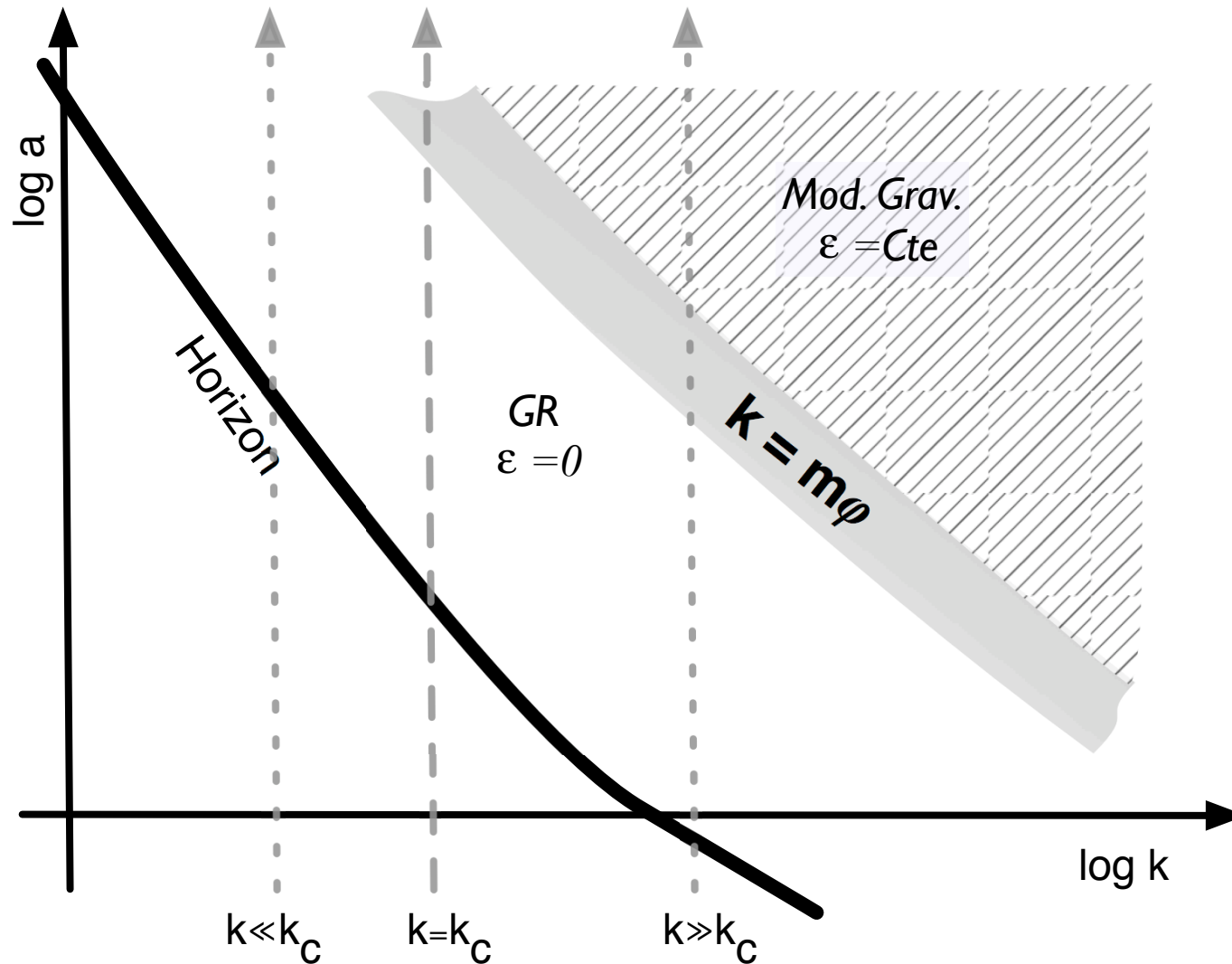


FIG. 1: Allowed parameter space for the environmentally dependent dilaton model. The shaded region is that where the presence of our galaxy is sufficient to ensure that the local value of the fifth force coupling, α , is smaller than the Cassini probe upperbound of 10^{-5} . We have modelled the galaxy as a spherical dark matter halo with NFW profile. We have taken typical values for the NFW model parameters for our galaxy: $r_{\text{vir}} = 267 \text{ kpc}$, $c = 12.0$, $M_{\text{v}} = 0.91 \times 10^{12} M_{\odot}$. We take the galactocentric radius of the solar system, r_{\odot} to be $r_{\odot} \approx 8.3 \text{ kpc}$. These choices correspond to $\Phi(r_{\odot}) = 1.02 \times 10^{-6}$ and $\rho(r_{\odot}) = 0.22 \text{ GeV cm}^{-3}$. This value for $\rho(r_{\odot})$ limits $\lambda < 170$, and we have plotted the constraints on A_2 for $\lambda \in [1, 170]$. Very similar bounds on A_2 result for different realistic models of the galactic halo.

Evolution of structure: from GR to modified gravity dynamics



A new Euler equation (up to second order)

$$\frac{1}{H}\dot{\theta}^{(2)} + \left(2 + \frac{\dot{H}}{H^2}\right)\theta^{(2)} + \frac{3}{2}\Omega_m(1 + \epsilon(k))\delta_m^{(2)} = -\beta(\mathbf{k}_1, \mathbf{k}_2)\theta^2 - [\mathcal{S}_{\text{Eul.}}(\mathbf{k}_1, \mathbf{k}_2) + \mathcal{S}_{\text{Intr.}}(\mathbf{k}_1, \mathbf{k}_2)](\delta_m^{(1)})^2$$

$$\mathcal{S}_{\text{Eul.}}(\mathbf{k}_1, \mathbf{k}_2) = \frac{(\mathbf{k}_2 \cdot \mathbf{k})}{k_1^2} \frac{a^2 m^2(\bar{\phi})}{k_2^2} S(k_1)\eta(k_2)$$

$$\mathcal{S}_{\text{Intr.}}(\mathbf{k}_1, \mathbf{k}_2) = \frac{a^2 m^2(\bar{\phi})}{k_2^2} S(k)\tilde{\eta}(k_2) + \frac{a^2 m^2(\bar{\phi})}{k_1^2} \frac{a^2 m^2(\bar{\phi})}{k_2^2} S(k_1)S(k_2)\mu(k)$$

$$\eta(k) = S(k) \frac{H^2}{m^2(\bar{\phi})} \frac{d(\beta_{\text{eff}}(\phi))}{k(\bar{\phi})d\phi}, \quad \tilde{\eta}(k) = S(k) \frac{H^2}{m^2(\bar{\phi})} \frac{d(A(\phi)\beta_{\text{eff}}(\phi))}{k(\bar{\phi})d\phi} \quad (\text{negligible in } \lambda \rightarrow \infty \text{ limit})$$

$$\mu(k) = \frac{S(k)}{3\Omega_m} \frac{H^2}{m^4(\bar{\phi})} \frac{d^3 V_{\text{eff}}}{2M_{\text{Pl}}^2 d\varphi^3} \quad (\text{negligible in } \lambda \rightarrow 0 \text{ limit})$$

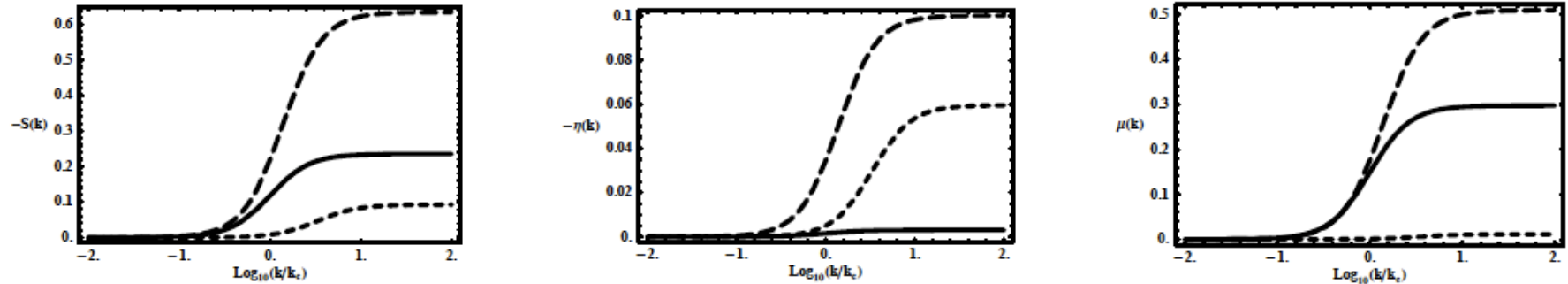
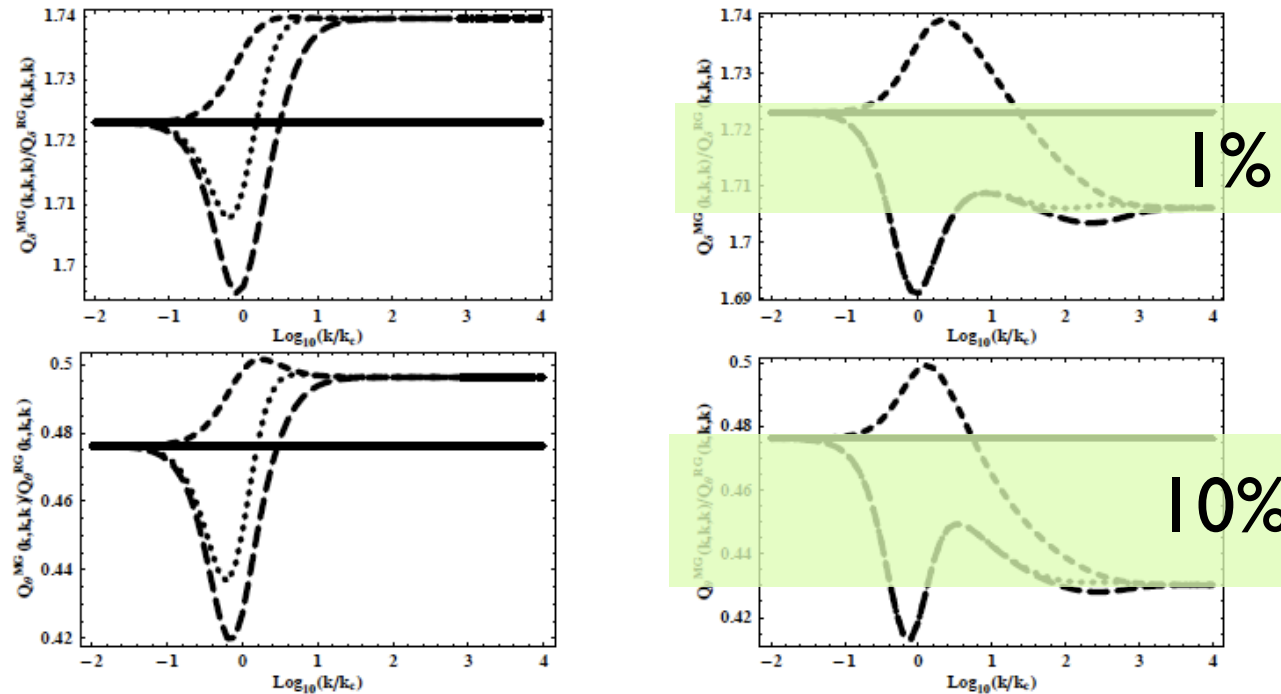


FIG. 5: Dependence on k of the parameters $S(k)$, $\eta(k)$ and $\mu(k)$ for $\eta = 0$ (solid lines), $\eta = -1$ (long dashed) and $\eta = -2$ (short dashed). Note that for the adopted parameters $\eta(k)$ and $\tilde{\eta}(k)$ are undistinguishable.

Bispectra (equilateral configurations)



- Similar effects (maybe slightly smaller) were found by Chan and Scoccimarro in case of the DGP model (where small scale GR is recovered through the Vainshtein mechanism).

Robust features are expected to be seen in large-scale structure observations. *Changing the strength/form of gravity laws is our best chance to induce significant (although mild) changes in the shape/amplitude of the observable bispectra.*

Conclusions

- New methods are being developed, still in progress
 - *RPT, Gamma-expansion, closure theory, time-flow RG, but also with an effective fluid approach has been proposed as a possible route to such calculations (Baumann et al., '10);*
 - *Which approach is the "best" (if any) is not clear yet;*
- Important cross-checks with N-body codes (for various models);
- An interesting play-ground for theoretical physicists;
- Maybe our best chance to unambiguously grasp the nature of dark energy (in particular through detailed analysis of 3-pts functions)